Talanta 104 (2013) 204–211

Contents lists available at SciVerse ScienceDirect

Talanta

journal homepage: www.elsevier.com/locate/talanta

A novel composite film derived from cysteic acid and PDDA-functionalized graphene: Enhanced sensing material for electrochemical determination of metronidazole

Weilu Liu [a], Jianfu Zhang [b], Cong Li [a], Liu Tang [a], Zhiquan Zhang [a,*], Ming Yang [c,**]

[a] College of Chemistry, Jilin University, Changchun 130012, PR China
[b] State Key Laboratory of Supramolecular Structure and Materials, College of Chemistry, Jilin University, Changchun 130012, PR China
[c] Department of Breast Surgery, First Hospital, Jilin University, Changchun 130021, PR China

ARTICLE INFO

Article history:
Received 2 August 2012
Received in revised form
6 November 2012
Accepted 8 November 2012
Available online 17 November 2012

Keywords:
Graphene
Cysteic acid
Electrochemical sensor
Metronidazole

ABSTRACT

A novel composite film derived from cysteic acid and poly(diallydimethylammonium chloride)-functionalized graphene (PDDA-GN) was employed as an enhanced electrode material for ultrasensitive determination of metronidazole. The cysteic acid/PDDA-GN composite film was prepared by the electrochemical grafting of cysteic acid onto the PDDA-GN coated glassy carbon electrode (GCE). The cyclic voltammetry investigations reveal that the peak current of metronidazole reduction at the cysteic acid/PDDA-GN/GCE was remarkably enhanced compared to the bare GCE, the cysteic acid/GCE and the PDDA-GN/GCE. This result implies the synergistic electrocatalytic effect of cysteic acid and PDDA-GN. The fabricated sensor shows linear response to metronidazole in the ranges of 10 nM–1 μM and 70 μM–800 μM, with a detection limit of 2.3 nM (S/N=3). The heterogeneous electron transfer rate constant and the diffusion coefficient of metronidazole were further evaluated by rotating disk electrode experiments. Moreover, we applied the present method to the determination of metronidazole in urine and lake water with satisfactory results.

1. Introduction

Metronidazole, a synthetic nitroimidazole medication introduced in 1959 (Scheme 1) [1], has a broad spectrum of activity against parasitic and bacterial infections. Nowadays, it is widely used for the treatment of diseases, including trichomonas, vincent's organisms, anaerobic bacteria, giardias and amebiasis [2]. However, metronidazole has been shown to cause cancer in experimental animals according to the International Agency for Research on Cancer (IARC) [3]. Although the evidence is insufficient to consider metronidazole as a human carcinogen, the debates regarding the safety of metronidazole have never been stopped [4–11]. Due to its potential carcinogenic properties, metronidazole is banned in Europe for veterinary use in the feed of animals by Council Regulation 613/98/EEC [12]. In view of the above, the accurate and sensitive determination of metronidazole in various samples is meaningful for food security, human health and investigations on the biological toxicity of metronidazole. Several methods such as titrimetry [13], spectrophotometry [14,15], thin-layer chromatography [16], gas chromatography [17], high-performance liquid chromatography [18] electrophoresis [19] and electroanalytical technique [20,21] have been applied to the determination of metronidazole. Among these methods mentioned above, electroanalytical technique is more attractive because of its high sensitivity, simplicity, fast response, and cheap equipment. On the other hand, the structure of metronidazole contains a nitro group, which is an active reducible center for electrochemical sensing. Nevertheless, the electrochemical reduction of metronidazole at a bare electrode is generally difficult owing to the poor reproducibility and sensitivity. The recent progress in nanoscience and nanotechnology can act as new elements for the electroanalytical technique in terms of accelerating the electron transfer between electrode and probe molecules, and enhancing sensitivity and selectivity. Typical instances are carbon nanotubes [22,23], carbon-fiber microdisk electrode [24,25], pretreated gold electrode [26], and molecularly imprinted polymer-carbon paste electrode [27]. All these sensors indicated that nanostructure materials and electrodes play an important role on the effective detection of metronidazole. Therefore, exploring new nanostructures for electroanalytical applications is highly meaningful and has been a challenging topic.

Graphene, a "rising" star material, has received enormous attention due to its remarkable electronic, optical and thermal properties, since it was first reported in 2004 [28–31]. Graphene and graphene

* Corresponding author. Fax: +86 431 85168399.
** Corresponding author.
E-mail addresses: zzq@jlu.edu.cn (Z. Zhang), yangming1967@163.com (M. Yang).

0039-9140/$ - see front matter © 2012 Elsevier B.V. All rights reserved.
http://dx.doi.org/10.1016/j.talanta.2012.11.013

based nanocomposites have exhibited desirable performance in the electroanalytical applications owing to its large surface area, high electrocatalytic activity, and conductivity [32–36]. Generally, chemical reduction of exfoliated graphene oxide (GO) is an efficient method for the large-scale production of graphene in low cost. The reagents used for the reduction of GO are hydrazine, dimethylhydrazine, hydroquinone, and $NaBH_4$, which are either highly toxic or explosive [37,38]. Furthermore, graphene has a tendency to agglomerate irreversibly through van der Waals interactions [39]. As a consequence, great efforts have been devoted to addressing these issues. Several mild and environmental friendly reagents such as sugar [40], ascorbic acid [41], and dopamine [42] have been employed as alternative reduction reagents. However, all these methods suffer from long time reaction or low dispersibility of graphene in aqueous solution. Recently, a satisfactory result has been achieved by using poly(diallydimethylammonium chloride) (PDDA), a positively charged polyelectrolyte, to prepare graphene from exfoliated GO [43,44]. The use of PDDA both as a reducing agent and a stabilizer resulted in the successful reduction of GO and well-dispersed graphene in aqueous solution. Interestingly, the positively charged PDDA-functionalized graphene (PDDA-GN) has been employed as a matrix to anchor some negatively charged materials for fabricating multifunctional and application-directed composites [45,46]. Meanwhile, cysteic acid is a unique molecular containing negatively charged sulfonate group. Fujishima's group [47] and Oliveira-Brett's group [48] have reported that cysteic acid can be synthesized by electrochemical oxidation of disulfide molecules (L-cystine), and an electroactive and strongly adsorbed cysteic acid layer was formed on the glassy carbon electrode (GCE) surface after the oxidation reaction. Hu's group [49,50] has demonstrated that cysteic acid plays an important role in the electrochemical sensing of several drugs due to its excellent adsorbability and biocompatibility. Therefore, the combination of PDDA-GN and cysteic acid will produce a novel composite with both the excellent electrical properties of graphene and the special features of cysteic acid.

In this work, a sensing platform for ultrasensitive determination of metronidazole was constructed based on the cysteic acid/PDDA-GN composite film. Herein, a facile microwave-heating procedure was used for the preparation of well-dispersed PDDA-GN. By employing this method, the reduction time was shortened to only eight minutes. The as-prepared PDDA-GN was cast on GCE for fabricating the PDDA-GN/GCE. Cysteic acid was then electrochemically grafted onto the PDDA-GN/GCE by the electrochemical oxidation of L-cystine, for fabricating the cysteic acid/PDDA-GN/GCE (Scheme 2). The electrochemical reduction of metronidazole at the cysteic acid/PDDA-GN/GCE shows higher signals than those at the bare electrode, the cysteic acid/GCE, and the PDDA-GN/GCE, revealing the excellent electrocatalytic activity of the composite film. More interestingly, the detection limit of the as-prepared metronidazole sensor is as low as 2.3 nM (S/N=3). Therefore, this facile strategy provided us a "green" and low cost approach to fabricate a graphene based biocompatible composite film, which should be a promising candidate for electrochemical sensing and many other technological applications.

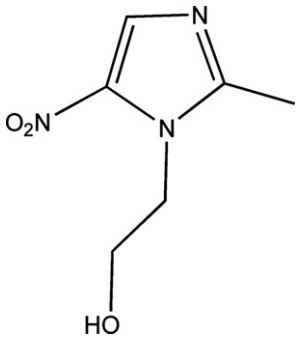

Scheme 1. The structure of metronidazole.

2. Experiments

2.1. Reagents and apparatus

Natural graphite was purchased from Tingdao Hengrui Industrial, China. PDDA (M_w=400,000–500,000, 20% in water) and L-cystine was obtained from Aldrich. Metronidazole (99.8%) was purchased from Aladdin Reagent, China. $K_3Fe(CN)_6$, $K_4Fe(CN)_6$ and all the

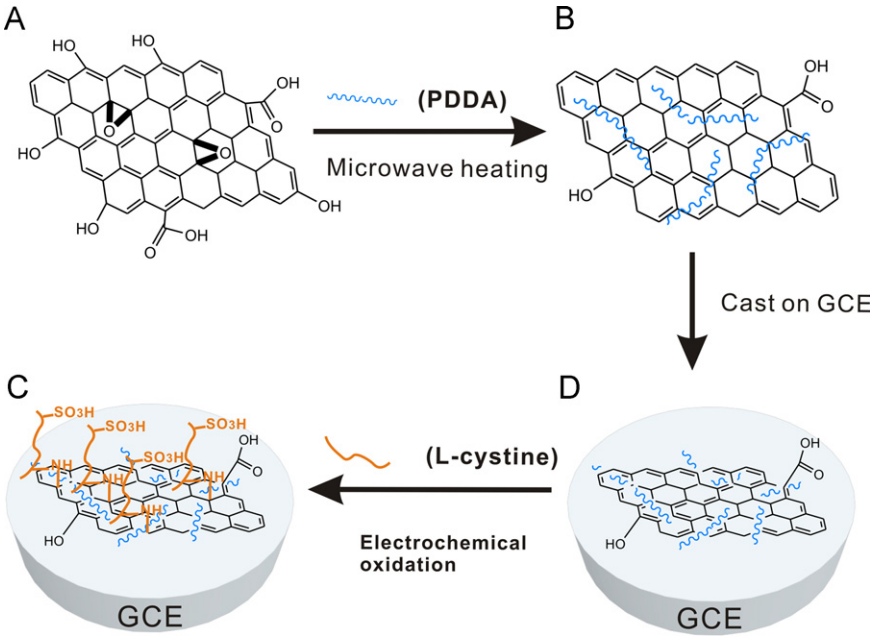

Scheme 2. The procedure for fabricating the cysteic acid/PDDA-GN/GCE. (A) GO, (B) PDDA-GN, (C) PDDA-GN/GCE and (D) cysteic acid/PDDA-GN/GCE

other chemicals are analytical grade from Shanghai Chemical Factory, China. Aqueous solutions were prepared with three distilled water.

The electrode materials were characterized by atomic force microscopy (AFM, Nanoscope IIIa Multimode, Digital Instruments, Santa Barbara, CA), scanning electron microscopy (SEM, Hitachi S-4800), X-ray photoelectron spectroscopy (XPS, AlKα radiation, ESCALAB-MKII 250 photoelectron spectrometer, VG Co.), X-ray diffraction (XRD, CuKα radiation, D/max2550VB X-ray diffractometer, Rigaku), Ultraviolet absorption spectroscopy (UV, UV-1700 Shimidazule), and Raman spectroscopy (solid-state laser at 532 nm radiation, Renishaw inVia Raman Microscope, UK).

2.2. Preparation of PDDA-GN

First, graphene oxide (GO) was synthesized from natural graphite powder by the modified Hummers method [51,52]. Then, PDDA (20% in water, 0.2 ml) was added into the homogeneous GO dispersion (0.5 mg/mL, 20.0 mL). After being sonicated for 30 min, the solution was placed in a household microwave oven for 8 min (power: 600 W. Notice: after continuous heating for 2 min, the microwave oven should stop for a 2-min rest). The product was isolated, and the residual PDDA was removed by centrifugation at 10,000 rpm for 20 min, followed by consecutive washing/centrifugation cycles two times with water. The collected product was redispersed readily in water/ethanol mixture to produce a colloidal PDDA-GN suspension.

2.3. Preparation of cysteic acid/PDDA-GN/GCE.

Prior to the modification, the GCE was polished with 1, 0.3 and 0.05 μm alumina slurry and rinsed thoroughly with water between each polishing step. Then, it was washed successively with 1:1 nitric acid, acetone and water in an ultrasonic bath and dried under a stream of nitrogen. The PDDA-GN suspension (0.5 mg/ml, 3 μL) was carefully cast on the cleaned GCE surface. After the modified GCE was dried, it was rinsed thoroughly with water, and the PDDA-GN/GCE was obtained. The PDDA-GN/GCE was then immersed into a deoxygenated electrolyte solution containing 10 mM L-cystine and 0.1 M H_2SO_4. By scanning the potential from -1 V to $+2$ V for ten cycles, the cysteic acid/PDDA-GN/GCE was obtained. For control experiment, the cysteic acid/GCE was obtained using a cleaned bare GCE in the same electrolyte and the same electrochemical parameters above.

2.4. Electrochemical measurement

Electrochemical experiments were performed on a CHI-920c workstation (CH Instruments). A three-electrode cell was employed. A glassy carbon electrode (3 mm diameter) was used as the working electrode, a platinum wire as the counter electrode, and an Ag/AgCl wire (KCl saturated) as the reference electrode. Before cyclic voltammetry (CV) and linear sweep voltammetry (LSV) determination of metronidazole, the BR buffer solution was deoxygenated by bubbling nitrogen gas for 20 min. Electrochemical impedance spectroscopy (EIS) measurements were carried out under an open-circuit voltage, with the frequency range of 0.01–100 000 Hz and the signal amplitude of 5 mV. Rotating disk electrode (RDE) experiments were performed on a BAS RDE-2 electrode using the LSV sweep rate of 5 mV s^{-1}.

3. Results and discussion

3.1. Characterization of the electrode material

3.1.1. PDDA-GN

Microwave irradiation has been proven to be a promising approach for rapid volumetric heating, which shortens the reaction time from several hours to a few minutes with enormous energy savings and cleanliness [53–56]. Herein, PDDA-GN was facilely prepared through a microwave-assisted heating procedure using PDDA both as a reducing reagent and stabilizer. After eight minutes of reduction, the UV absorption peak of the GO dispersion at 230 nm shifts to 265 nm (Fig. 1A), indicating that the electronic conjugation within the PDDA-GN nanosheets was restored upon the reduction procedure [57].

We further characterized the as-prepared PDDA-GN by XRD, Raman spectroscopy and AFM. Fig. 1B shows the XRD patterns of the pristine graphite, GO, and PDDA-GN. A dominant peak is observed at $2\theta=26.5$ °C(002) from graphite powder, corresponding to an interlayer space (d-spacing) of 0.34 nm (curve a). Compared with the pristine graphite, the diffraction peak of exfoliated GO appears at $2\theta=9.8$ °C (002) with interlay space (d-spacing) of 0.86 nm (curve b). This increased d-spacing value of GO is a result of the introduction of oxygenated functional groups on carbon sheets. After microwave-assisted reduction with PDDA, the diffraction peak at $2\theta=9.8^\circ$ disappears and a broad peak around 22.0° is observed (curve c). This broad peak can be assigned to the hexagonal graphite structure C (002), and confirms the reduction of GO and the exfoliation of the layered PDDA-GN [56,58].

Raman spectroscopy is a useful nondestructive method to characterize the structure and quality of carbonaceous materials, particularly for distinguishing ordered and disordered structures. G band is usually assigned to the E_{2g} phonon of C sp^2 atoms, while D band is a breathing mode of κ-point phonons of A_{1g} symmetry [59]. Raman spectroscopy for both GO (Fig. 1C, curve a) and PDDA-GN (Fig. 1C, curve b) exhibit two remarkable peaks at around 1350 and 1600 cm^{-1}, which assign to the well-defined D band and G band, respectively. The frequency of the D band and G band in PDDA-GN are similar to those observed in GO. However, PDDA-GN has an obvious increased D/G intensity ratio compared with GO. This change indicates a decrease in the size of the in-plane sp^2 domains and a partially ordered crystal structure of PDDA-GN [60]. Therefore, the data from UV spectroscopy, XRD, and Raman spectroscopy clearly demonstrate that GO were successfully reduced to PDDA-GN.

The morphology of PDDA-GN was further characterized by AFM. PDDA-GN appears in the form of a number of flake-like nanostructures as shown in Fig. 2A. As shown the section analysis in Fig. 2B, the thickness of PDDA-GN is between 1 and 2 nm, which is the typical characteristics of single-layer graphene [61]. Interestingly, this PDDA-GN dispersion was stable and no precipitates were observed after stored for three months. Thus, this positively charged and well-dispersed PDDA-GN was used for grafting cysteic acid.

3.1.2. Cysteic acid/PDDA-GN composite on GCE

Cysteic acid was electrochemically grafted on PDDA-GN by cyclic voltammetry oxidation of cystine. The dominant oxidation peak at 1.53 V in Fig. S1 is responsible for the oxidation of disulfide bond to sulfonate group, and indicates the formation of cysteic acid [47,48]. We further characterized the as-prepared cysteic acid/PDDA-GN composite using XPS, EIS and SEM. Fig. 3A shows the XPS in the S 2p region. The binding energy peak at ~167.8 eV corresponds to the sulfur atom in the sulfonic group of cysteic acid [62]. Fig. 3B shows the XPS in the N 1s region.

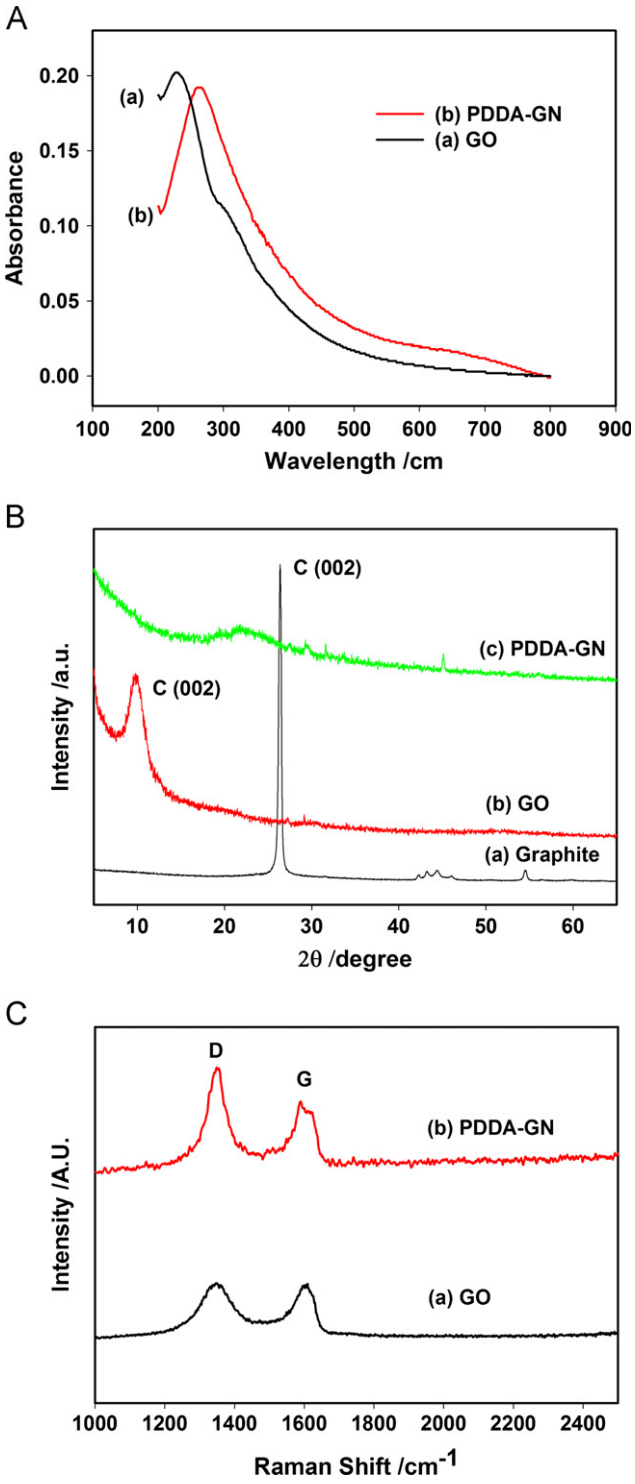

Fig. 1. (A) UV absorption spectroscopy of GO (a) and PDDA-GN (b). (B) XRD patterns of graphite (a), GO (b), and PDDA-GN (c). (C) Raman spectroscopy of GO (a) and PDDA-GN (b).

The binding energy peak at ~399.5 eV is attributed to the formation of a carbon-nitrogen bond between the amine cation radical and the carbon atom of PDDA-GN [63,64]. The XPS analysis indicates that cystine was successfully oxidized to cysteic acid, and the resulting cysteic acid was grafted to PDDA-GN through a nitrogen–carbon bond. On the other hand, the electrostatic attraction between the positively charged PDDA-GN and the negatively charged cysteic acid (sulfonate group) also contributes to the formation of the composite.

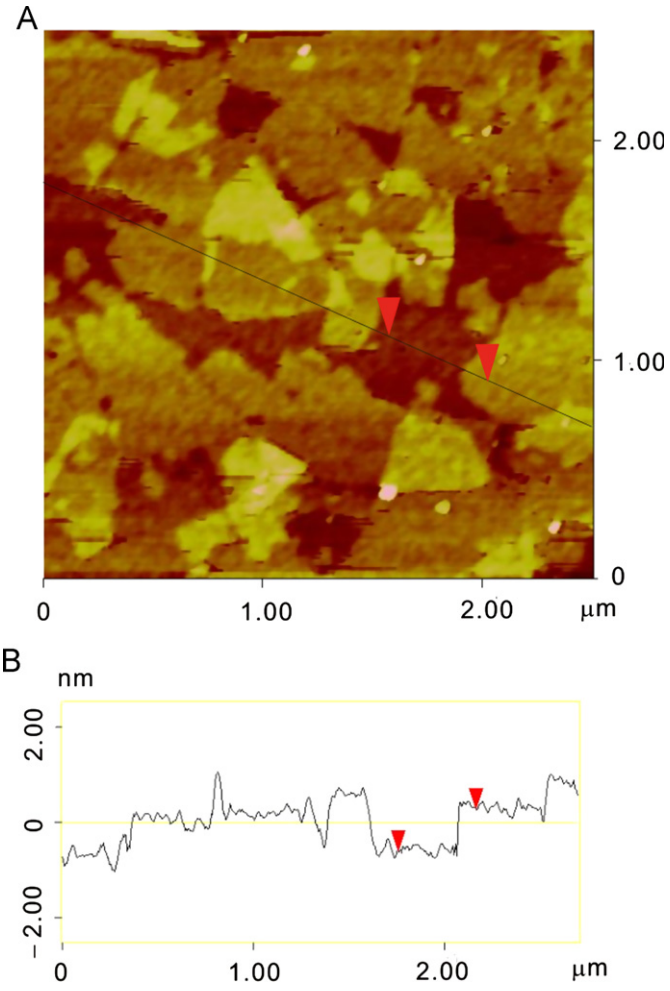

Fig. 2. (A) AFM image of PDDA-GN. (B) The cross section identified by the line in (A) shows the height of PDDA-GN.

EIS is a valid method to monitor the features of a surface-modified electrode and can give information on the impedance changes of the electrode surface during the modification process. Fig. 3C shows the Nyquist plots of the EIS at the bare GCE (a), the cysteic acid/GCE (b), and the cysteic acid/PDDA-GN/GCE in the presence of 10 mM $Fe(CN)_6^{3-/4-}$ and 0.1 M KCl. The charge-transfer resistance (R_{ct}) at the electrode surface is equal to the semicircle diameter in the plot and can be deduced by fitting the impedance data using the equivalent circuit (inset of Fig. 3C). For the bare GCE (curve a), the R_{ct} value was estimated to be 113.5 Ω. The R_{ct} value increases to 1196.0 Ω (curve b), due to the immobilization of cysteic acid on GCE. After doping PDDA-GN, the R_{ct} value decreases dramatically to 534.4 Ω (curve c), implying PDDA-GN plays an important role in accelerating the electron transfer between electrode and probe molecules. These EIS results demonstrated the successful immobilization of cysteic acid/PDDA-GN composite and its high charge transfer ability.

The morphology of the cysteic acid/PDDA-GN composite on the GCE was characterized by SEM. Fig. 4 reveals the rough surface of the GCE modified with the typical crumpled and wrinkled cysteic acid/PDDA-GN composite. The active electrode surface area was estimates as 0.216 cm^2 by chronoamperometry using 1 mM $Fe(CN)_6^{3-}$ in 0.1 M KCl as the model probe, based on the Conttrell equation [65]. This surface area is obviously larger than the geometry area of 0.07 cm^2, and it is one of the favorable elements for electrochemical sensing applications.

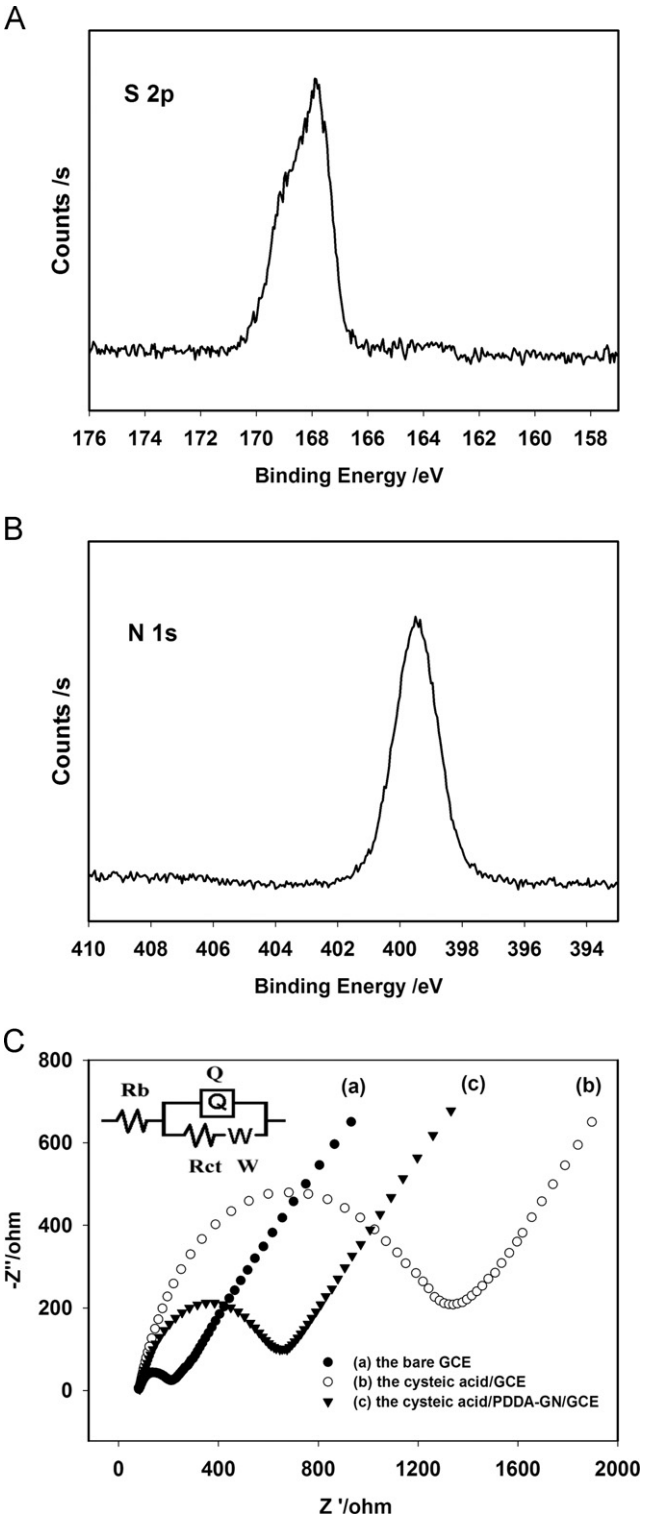

Fig. 3. (A, B) XPS spectroscopy of the cysteid acid/PDDA-GN composite in the S 2p region (A) and N 1s region (B). (C) Nyquist plots of 10 mM $Fe(CN)_6^{3-/4-}$ containing 0.1 M KCl solution at the bare GCE (a), the cysteic acid/GCE (b) and the cysteic acid/PDDA-GN/GCE (c). The frequency range is from 0.1 Hz to 100 kHz. Inset is the equivalent circuit. R_b: bulk resistance, R_{ct}: charge transfer resistance, Q: constant phase element(CPE), W: Warburg.

3.2. Electrochemical behaviors of metronidazole

Fig. 5 shows the cyclic voltammograms of 300 μM metronidazole at the bare GCE (a), the cysteic acid/GCE (b), the PDDA-GN/GCE (c) and the cysteic acid/PDDA-GN/GCE (d) in BR (pH 8.0)

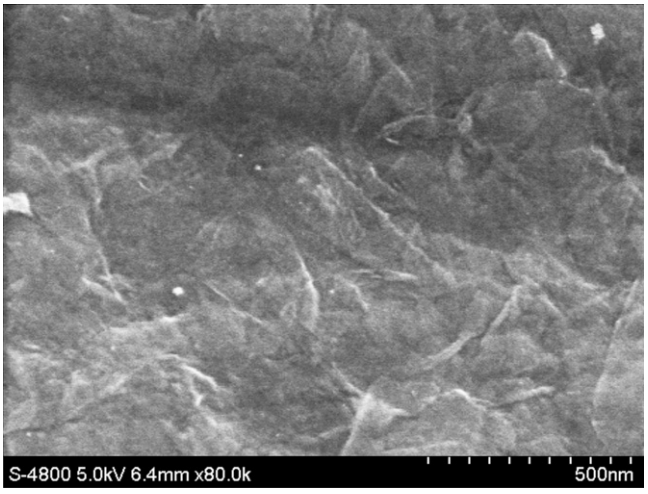

Fig. 4. SEM image of the cysteic acid/PDDA-GN composite on GCE surface.

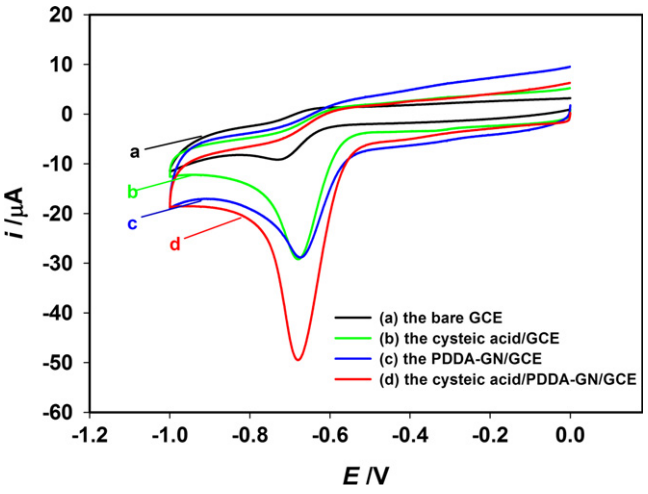

Fig. 5. Cyclic voltammograms of 300 μM metronidazole in BR (pH 8.0) solution at the bare GCE (a), the cysteic acid/GCE (b), the PDDA-GN/GCE (c), and the cysteic acid/PDDA-GN/GCE (d). Scan rate: 100 mV s^{-1}.

solution. Well defined reduction peaks are observed within the potential window from 0 to −1.0 V, and no oxidation peaks are visible in the reverse scan, suggesting that metronidazole undergo an irreversible reduction process on the electrodes. The peak current and peak potential of metronidazole at the bare GCE are 6.7 μA and −0.732 V, respectively. At the cysteic acid/GCE, the peak current increased by a factor of 3.8 compared to the bare GCE. This enhanced signal may be attributed to the strong H-bonding interaction between the hydroxyl groups in metronidazole and the functional groups (sulfonate and carboxyl group) in cysteic acid. This interaction can improve the accumulation of metronidazole on the electrode surface, which is favorably for the electrochemical reduction reaction. At the PDDA-GN/GCE, the peak current increased by a factor of 3.0 relatively to the bare GCE. This data implies that PDDA-GN can promote metronidazole reduction due to its excellent conductivity and large surface area. Interestingly, a largest peak current (6.3 times of the one at the bare GCE), was observed at the cysteic acid/PDDA-GN/GCE. This obvious enhancement can be ascribed to the synergistic effect of cysteic acid and PDDA-GN. More importantly, we found that the overpotentials at the modified electrodes were about 60 mV lower than that at the bare GCE. Therefore, the excellent performance of cysteic acid/PDDA-GN composite makes it a better choice for the electrochemical sensing of metronidazole.

3.3. Effect of pH and scan rate

The effect of solution pH on the electrochemical behavior of metronidazole at the cysteic acid/PDDA-GN/GCE was investigated with BR solution in the pH range from 3.0 to 10.0 (Fig. 6A). The inset (1) shows that the peak current increased by varying pH from 3.0 to 8.0, and decreased slightly when the pH values exceeded 8.0. The inset (2) reveals that the peak potentials moved to more negative values as the increase of pH from 3.0 to 8.0, and kept almost constant from pH 8.0 to 10.0. As a consequence, BR solution of pH 8.0, which leads to the best metronidazole response, was used for all the voltammetric determinations.

The effect of scan rates on the peak currents of metronidazole at the cysteic acid/PDDA-GN/GCE was investigated by cyclic voltammetry (Fig. 6B). It is observed that the peak potentials shift slightly as the increase of scan rate. At the same time, the reduction peak currents increased linearly with the square root of scan rates in the range of 10–310 mV s^{-1}, with a linear regression equation of i_p (A)$=1.038\times10^{-6}$–$3.939\times10^{-3}\,\nu^{1/2}$ (V s^{-1})$^{1/2}$ ($R^2=0.999$). This indicates that the reduction of metronidazole is a diffusion-controlled process, which is the ideal case for quantitative determination.

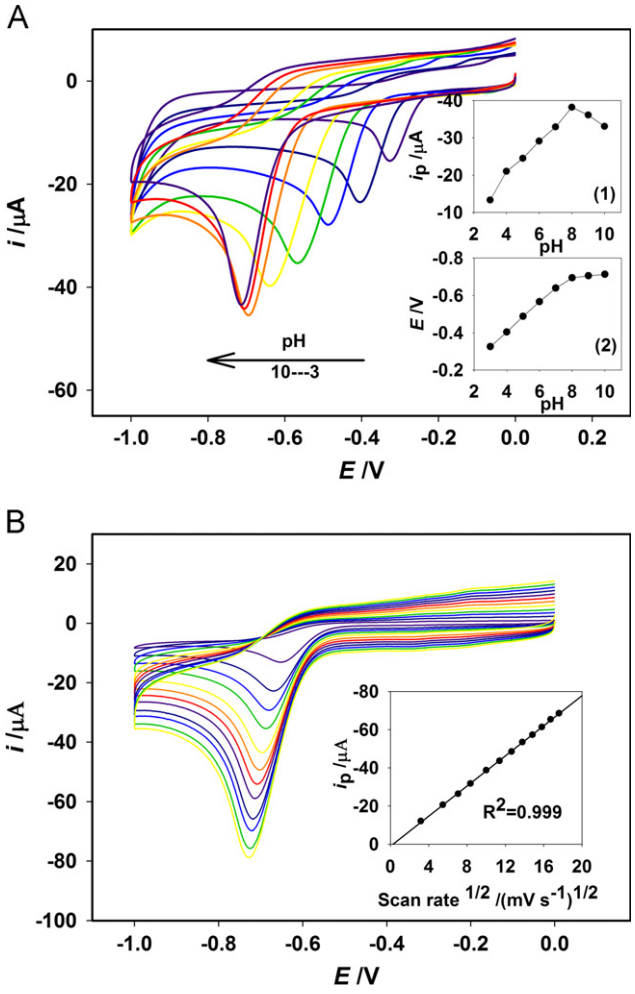

Fig. 6. (A) Cyclic voltammograms of 300 μM metronidazole at the cysteic acid/PDDA-GN/GCE in BR solution with different pH values (from 3.0 to 10.0). Scan rate: 100 mV s^{-1}. Inset 1: the plot of peak current versus pH values, inset 2: the plot of peak potential versus pH values. (B) Cyclic voltammograms of 300 μM metronidazole at the cysteic acid/PDDA-GN/GCE in BR (pH 8.0) solution with different potential scan rate (10, 30, 50, 70, 100, 130, 160, 190, 220, 250, 280, and 310 mV s^{-1}). Inset: the plot of peak currents versus square root of scan rates.

3.4. Rotating disk electrode investigation

Rotating disk electrode (RDE) technique is an effective method for obtaining the kinetic information of electrode reactions with high stability and accuracy. Fig. 7 shows the RDE response at the cysteic acid/PDDA-GN/GCE with different metronidazole concentrations and different rotation speeds. Steady-state character of the measured currents was ensured by controlling the sweep rate at 5 mV s^{-1}. Levich plots in Fig. 7A shows that the limiting currents increased linearly with the square root of rotation speed at lower rotation rates, suggesting that the limiting currents are controlled by mass-transport. While the Levich plots deviated from linearity at higher rotating rates, indicating a kinetic limitation. In this case, the Koutecky–Levich equation [65] was used to determine the heterogeneous electron transfer rate constant. The limiting current is given by:

$$i_{lim}^{-1}=i_{Lev}^{-1}+i_K^{-1} \quad (1)$$

where, i_{Lev} is the Levich current, i_K is the kinetic current. It can be defined by:

$$i_{Lev}=0.62nFAD^{2/3}\upsilon^{-1/6}\omega^{1/2}C_O \quad (2)$$

$$i_k=nFAC_Ok \quad (3)$$

where n is the number of electron transferred ($n=4$ according to the previous reports [20,22]), F (96485.3 C mol^{-1}) is the Faraday

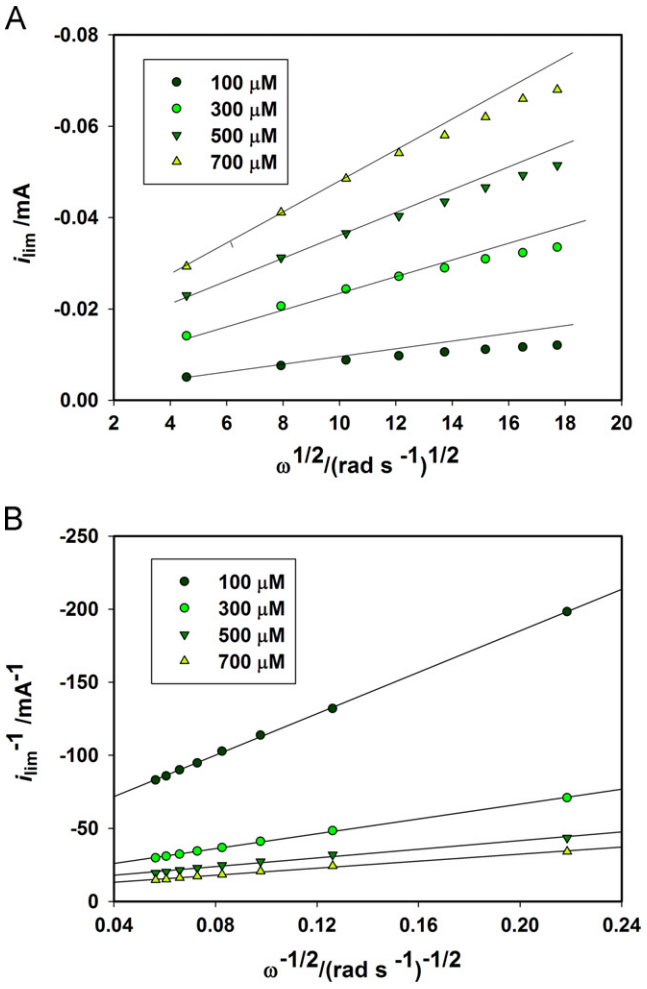

Fig. 7. (A) Levich plots (i_{lim} versus $\omega^{1/2}$) and (B) Koutecky–Levich plots (i_{lim}^{-1} versus $\omega^{-1/2}$) at the cysteic acid/PDDA-GN/GCE with different concentrations of metronidazole (100, 300, 500, 700 μM) and different rotation speeds (200, 600, 1000, 1400,1800, 2200, 2600, and 3000 rpm).

constant, A (0.216 cm^2) is the electrochemical active electrode area, D ($cm^2\ s^{-1}$) is the diffusion coefficient, υ (0.01 $cm^2\ s^{-1}$) is the kinematic viscosity, ω (rad s^{-1}) is the rotation rate, C_O is the bulk concentration (M), and k ($cm\ s^{-1}$) is the heterogeneous electron transfer rate constant.

Based on Koutecky–Levich equation, the plots (i_{lim}^{-1} versus $\omega^{-1/2}$) give straight lines in Fig. 7B. Using the intercept of the curves, the average k value in the metronidazole concentration range was calculated as 2.34×10^{-3} cm s^{-1}. Moreover, the diffusion coefficient of metronidazole can be obtained from the slope of curves. The average value was found to be 1.29×10^{-6} $cm^2\ s^{-1}$, which is close to the value in the previous study [66]. We suppose these kinetic parameters should be useful for the further development of high-performance metronidazole reduction catalysts, and for the investigation upon the physio-toxicity and potential carcinogenic property of metronidazole.

3.5. Determination of metronidazole by linear sweep voltammetry

Under the optimal conditions, linear sweep voltammetry (LSV) was performed at the cysteic acid/PDDA-GN/GCE for the determination of metronidazole. The LSV response to different concentrations of metronidazole is shown in Fig. 8. The reduction peak current is proportional to the concentration in the ranges of 10 nM–1 μM (Fig. 8A) and 70 μM–800 μM (Fig. 8B). The corresponding linear regression equations are i_p (μA)= −0.2527–0.4924 C (μM) (R^2=0.998) and i_p (μA)= −12.68–0.08427 C (μM) (R^2=0.994), respectively. The detection limit is estimated as 2.3 nM (S/N=3). Compared with the previous reports in Table 1, this work has wider linear range and lower detection limit. This interesting result further confirmed the synergistic effect of PDDA-GN and cysteic acid. Cysteic acid can increase the adsorptive site for metronidazole, while PDDA-GN can enhance the surface area and electric conductivity. These results indicate that the cysteic acid/PDDA-GN/GCE is a preferable sensing platform for the determination of metronidazole.

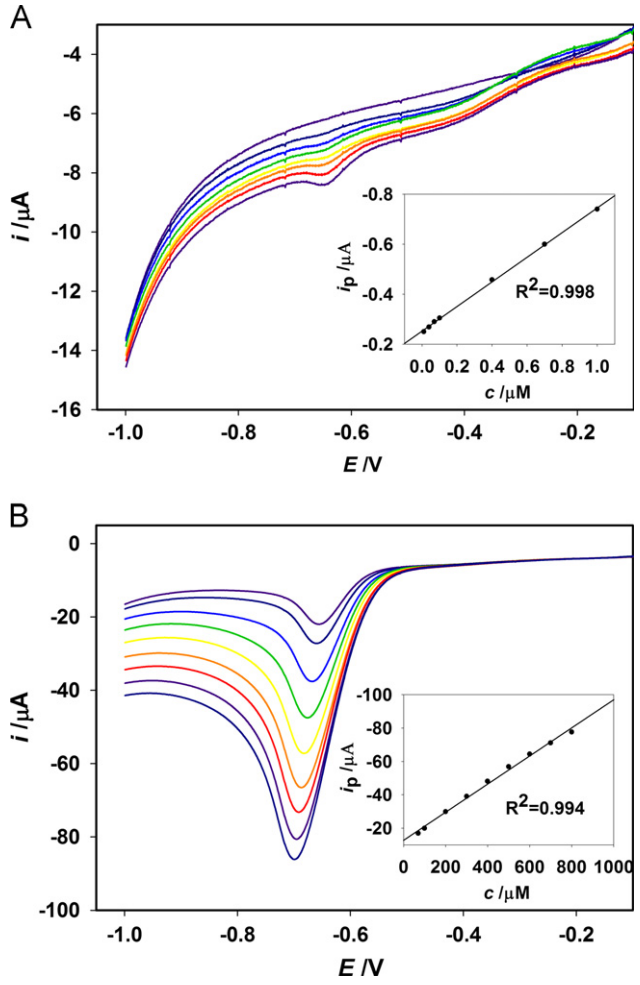

Fig. 8. LSV response at the cysteic acid/PDDA-GN/GCE for different concentrations of metronidazole in BR (pH 8.0) solutions. Scan rate: 100 mV s^{-1}. (A) From top to bottom, 0, 0.01, 0.04, 0.07, 0.1, 0.4, 0.7 and 1 μM. (B) From top to bottom, 70, 100, 200, 300, 400, 500, 600, 700, and 800 μM. Insets: the plots of peak current of metronidazole versus its concentrations.

3.6. Repeatability, stability and interferences

The repeatability of the cysteic acid/PDDA-GN/GCE was evaluated by measuring a 100 μM metronidazole solution for 15 successive times with the same electrode. The results revealed that the electrode possesses a satisfying repeatability with a relative standard deviation (RSD) of 3.26%. When detecting 100 μM metronidazole for several times in seven days, the electrode kept 95.4% of its initial current response. After the electrode was stored for two months at room temperature, only a small current decrease (about 5.2%) was observed. The influence of some common ions and organics on the determination of metronidazole was studied. It was found that the concentration of 1000 times of K^+, Na^+, Ca^{2+}, Mg^{2+}, Zn^{2+}, Cl^-, AC^-, $H_2PO_4^-$, HPO_4^{2-}, SO_4^{2-}, and 500 times of uric acid, dopamine, ascorbic acid did not affect the determination of metronidazole (signal change below 3%).

3.7. Analytical applications

The practical analytical utility of the modified electrode was evaluated by the determination of metronidazole in human urine and local lake water (South-Lake, Changchun, China). The samples were diluted 30-times with BR solution (pH 8.0) and determined by LSV technique. In Fig. S2, the modified electrode had no response when metronidazole was not added in the samples. After the samples were spiked with a certain amount of metronidazole, well-defined reduction peak were observed on the modified electrode. The standard addition method was used for calculating the metronidazole concentrations. The obtained results are summarized in Table 2. The recoveries of the sample are 96.8–103.8% and 102.6–104.1% for urine and lake water, respectively. The RSD are below 3.8%. Therefore, the sensing platform based on cysteic acid/PDDA-GN is reliable for the determination of metronidazole in practical samples.

Table 1
Analytical parameters of several electrodes for mentronidazole determination.

Electrode	Linear range (μM)	LOD (μM)	Ref.
Activated GCE	2–600	1.1	[20]
MWCNT[a]	0.025–10	0.006	[22]
SWCNT[b]	0.1–200	0.063	[23]
Carbon fiber microdisk electrode	1–22	0.5	[24]
Pretreated gold electrode	0.5–10 and 20–800	0.15	[26]
Gr-IL/GCE[c]	0.1–25	0.047	[67]
Metalloporphyrin CPE[d]	0.058–2900	0.058	[68]
Cysteic acid/PDDA-GN/GCE	0.01–1 and 70–800	0.0023	This work

[a] Multi-walled carbon nanotubes.
[b] Single-walled carbon nanotubes.
[c] Graphene-ionic liquid.
[d] Carbon paste electrode.

Table 2
Determination of metronidazole in practical samples.

Sample	Added (μM)	Found[a] (μM)	RSD (%)	Recovery (%)
Urine	90	87.1	2.6	96.8
Urine	120	124.6	3.1	103.8
Lake water	150	156.1	3.8	104.1
Lake water	180	184.6	2.9	102.6

[a] Average of three determinations.

4. Conclusions

A green, facile and low cost strategy was employed to fabricate a metronidazole sensor based on the cysteic acid/PDDA-GN composite film. The cysteic acid/PDDA-GN composite exhibited excellent electrocatalytic activity for the reduction of metronidazole owing to the synergistic effect of PDDA-GN and cysteic acid. The wide linear range, low detection limit, and good selectivity of the as-prepared sensor hold potential for the practical determination of metronidazole. Therefore, the high electrochemical performance and the biocompatibility of the cysteic acid/PDDA-GN composite make it a promising candidate for electrochemical sensor and further biosensor applications.

Acknowledgments

This work was supported by the NNSFC (no. 20605009) and Jilin University.

Appendix A. Supporting information

Supplementary data associated with this article can be found in the online version at http://dx.doi.org/10.1016/j.talanta.2012.11.013.

References

[1] C. Cosar, L. Julou, Ann. Inst. Pasteur 96 (1959) 238–241.
[2] P. Speelman, Antimicrob. Agents Chemother. 27 (1985) 227–229.
[3] IARC, International Agency for Research on Cancer, Lyon, France, (Suppl. 7), (1987), S250–S251.
[4] J.R. Krause, H.Q. Ayuyang, L.D. Ellis, Am. J. Gastroenterol. 80 (1985) 978–982.
[5] L. Dobias, M. Cerna, P. Rossner, R. Sram, Mutat. Res. 317 (1994) 177–194.
[6] A. Bendesky, D. Menendez, P. Ostrosky-Wegman, Mutat. Res. 511 (2002) 133–144.
[7] F.J. Roe, Surgery 93 (1983) 158–164.
[8] E. Bostofte, J.F. Bak, R. Hoier, Ugeskr. Laeger. 143 (1981) 2211–2214.
[9] M.E. Falagas, A.M. Walker, H. Jick, R. Ruthazer, J. Griffith, D.R. Snydman, Clin. Infect. Dis. 26 (1998) 384–388.
[10] C.M. Beard, K.L. Noller, W.M. O'Fallon, L.T. Kurland, D.C. Dahlin, Mayo Clin. Proc. 63 (1988) 147–153.
[11] C.A. Valdez, J.C. Tripp, Y. Miyamoto, J. Kalisiak, P. Hruz, Y.S. Andersen, S.E. Brown, K. Kangas, L.V. Arzu, B.J. Davids, F.D. Gillin, J.A. Upcroft, P. Upcroft, V.V. Fokin, D.K. Smith, K.B. Sharpless, L. Eckmann, J. Med. Chem. 52 (2009) 4038–4053.
[12] Council Regulation (EEC) 613/98, Off. J. Eur. Commun., (1998) L 82/14.
[13] P. Parimoo, J. Indian Chem. Soc. 65 (1988) 151–152.
[14] P. Parimoo, C.V.N. Prasad, R. Vineeth, J. Pharm. Biomed. Anal. 14 (1996) 289–393.
[15] P. Nagarajia, K.R. Sunitha, R.A. Vasatha, H.S. Yathirajan, J. Pharm. Biomed. Anal. 28 (2002) 527–535.
[16] P. Parimoo, P. Umapathi, N. Ravikumar, S. Rayasehar, Indian Drugs 29 (1992) 228–230.
[17] S.C. Bhatia, V.D. Shanbhag, J. Chromatogr. 305 (1984) 325–334.
[18] A. Turcant, A. Premel-Cabic, A. Caileux, P. Allain, Clin. Chem. 37 (1991) 1210–1215.
[19] W. Jin, W. Li, Q. Xu, Q. Dong, Electrophoresis 21 (2000) 1409–1414.
[20] S.A. Özkan, Y. Özkan, Z. Şentürk, J. Pharm. Biomed. Anal. 17 (1998) 299–305.
[21] M.A. La-Scalea, S.H.P. Serrano, I.G.R. Gutz, J. Braz. Chem. Soc. 10 (1999) 127–135.
[22] S. Lu, K. Wu, X. Dang, S. Hu, Talanta 63 (2004) 653–657.
[23] A. Salimi, M. Izadi, R. Hallaj, M. Rashidi, Electroanalysis 19 (2007) 1668–1676.
[24] P.N. Bartlett, E. Ghoneim, G. El-Hefnawy, I. El-Hallag, Talanta 66 (2005) 869–874.
[25] A. Guzmán, L. Agüí, M. Pedrero, P. Yáñez-Sedeño, J.M. Pingarrón, Electroanalysis 16 (2004) 1763–1770.
[26] B. Rezaei, S. Damiri, Electrochim. Acta 55 (2010) 1801–1808.
[27] M.B. Gholivand, M. Torkashvand, Talanta 84 (2011) 905–912.
[28] S. Chen, J.W. Liu, M.L. Chen, X.W. Chen, J.H. Wang, Chem. Commun. (Camb) 48 (2012) 7637–7639.
[29] K.S. Novoselov, A.K. Geim, S.V. Morozov, D. Jiang, Y. Zhang, S.V. Dubonos, I.V. Grigorieva, A.A. Firsov, Science 306 (2004) 666–669.
[30] J.G. Hu, F.H. Li, K.K. Wang, D.X. Han, Q.X. Zhang, J.H. Yuan, L. Niu, Talanta 93 (2012) 345–349.
[31] D.H. Wang, D.W. Choi, J. Li, Z.G. Yang, Z.M. Nie, R. Kou, D.H. Hu, C.M. Wang, L.V. Saraf, J.G. Zhang, I.A. Aksay, J. Liu, ACS Nano 3 (2009) 907–914.
[32] Y. Wang, Y. Li, L. Tang, J. Lu, J. Li, Electrochem. Commun. 11 (2009) 889–892.
[33] J. Lu, L.T. Drzal, R.M. Worden, I. Lee, Chem. Mater. 19 (2007) 6240–6246.
[34] S.J. Guo, D. Wen, Y.M. Zhai, S.J. Dong, E.K. Wang, Biosens. Bioelectron. 26 (2011) 3475–3481.
[35] M. Zhou, Y.M. Zhai, S.J. Dong, Anal. Chem. 81 (2009) 5603–5613.
[36] S.J. Guo, D. Wen, Y.M. Zhai, S.J. Dong, E.K. Wang, ACS Nano 4 (2010) 3959–3968.
[37] V.C. Tung, M.J. Allen, Y. Yang, R.B. Kaner, Nat. Nanotechnol. 4 (2009) 25–29.
[38] S. Stankovich, R.D. Piner, X.Q. Chen, N.Q. Wu, S.T. Nguyen, R.S. Ruoff, J. Mater. Chem. 16 (2006) 155–158.
[39] Y.Y. Liang, D.Q. Wu, X.L. Feng, K. Mullen, Adv. Mater. 21 (2009) 1679–1683.
[40] C.Z. Zhu, S.J. Guo, Y.X. Fang, S.J. Dong, ACS Nano 4 (2010) 2429–2437.
[41] J.L. Zhang, H.J. Yang, G.X. Shen, P. Cheng, J.Y. Zhang, S.W. Guo, Chem. Commun. 46 (2010) 1112–1114.
[42] L.Q. Xu, W.J. Yang, K.-G. Neoh, E.-T. Kang, G.D. Fu, Macromolecules 43 (2010) 8336–8339.
[43] S. Zhang, Y. Shao, H. Liao, M.H. Engelhard, G. Yin, Y. Lin, ACS Nano 5 (2011) 1785–1791.
[44] Z.-G. Le, Z. Liu, Y. Qian, C. Wang, Appl. Surf. Sci. 258 (2012) 5348–5353.
[45] D.B. Lu, Y. Zhang, L.T. Wang, S.X. Lin, C.M. Wang, X.F. Chen, Talanta 88 (2012) 181–186.
[46] Y.X. Fang, S.J. Guo, C.Z. Zhu, Y.M. Zhai, E.K. Wang, Langmuir 26 (2010) 11277–11282.
[47] C. Terashima, T.N. Rao, B.V. Sarada, Y. Kubota, A. Fujishima, Anal. Chem. 75 (2003) 1564–1572.
[48] T.A. Enache, A.M. Oliveira-Brett, Bioelectrochemistry 81 (2011) 46–52.
[49] C. Wang, Y. Mao, D. Wang, G. Yang, Q. Qu, X. Hu, Bioelectrochemistry 72 (2008) 107–115.
[50] C. Wang, X. Shao, Q. Liu, Q. Qu, G. Yang, X. Hu, J. Pharm. Biomed. Anal. 42 (2006) 237–244.
[51] W. Hummers, R. Offeman, J. Am. Chem. Soc. 80 (1958) 1339.
[52] N.I. Kovtyukhova, P.J. Ollivier, B.R. Martin, T.E. Mallouk, S.A. Chizhik, E.V. Buzaneva, A.D. Gorchinskiy, Chem. Mater. 11 (1999) 771–778.
[53] T. Lu, L. Pan, H. Li, G. Zhu, T. Lv, X. Liu, Z. Sun, T. Chen, D.H.C. Chua, J. Alloys Compd. 509 (2011) 5488–5492.
[54] A.V. Murugan, T. Muraliganth, A. Manthiram, Chem. Mater. 21 (2009) 5004–5006.
[55] M. Zhang, D. Lei, X. Yin, L. Chen, Q. Li, Y. Wang, T. Wang, J. Mater. Chem. 20 (2010) 5538–5543.
[56] H.M.A. Hassan, V. Abdelsayed, A.E.R.S. Khder, K.M. AbouZeid, J. Terner, M.S. El-Shall, S.I. Al-Resayes, A.A. El-Azhary, J. Mater. Chem. 19 (2009) 3832–3837.
[57] D. Li, M.B. Muller, S. Gilje, R.B. Kaner, G.G. Wallace, Nat. Nano 3 (2008) 101–105.
[58] M.J. McAllister, J.-L. Li, D.H. Adamson, H.C. Schniepp, A.A. Abdala, J. Liu, M. Herrera-Alonso, D.L. Milius, R. Car, R.K. Prud'homme, I.A. Aksay, Chem. Mater. 19 (2007) 4396–4404.
[59] F. Tuinstra, J.L. Koenig, J. Chem.Phys. 53 (1970) 1126–1130.
[60] S. Stankovich, D.A. Dikin, R.D. Piner, K.A. Kohlhaas, A. Kleinhammes, Y. Jia, Y. Wu, S.T. Nguyen, R.S. Ruoff, Carbon 45 (2007) 1558–1565.
[61] C.N.R. Rao, A.K. Sood, K.S. Subrahmanyam, A. Govindaraj, Angew. Chem. Int. Ed. 48 (2009) 7752–7777.
[62] R. Molina, J.P. Espinós, F. Yubero, P. Erra, A.R. González-Elipe, Appl. Surf. Sci. 252 (2005) 1417–1429.
[63] R.S. Deinhammer, M. Ho, J.W. Anderegg, M.D. Porter, Langmuir 10 (1994) 1306–1313.
[64] L. Zhang, X. Jiang, E. Wang, S. Dong, Biosens. Bioelectron. 21 (2005) 337–345.
[65] A.J. Bard, L.R. Faulkner, Electrochemical Methods, Fundamentals and Applications, Wiley, New York, 1980.
[66] X. Jiang, X. Lin, Bioelectrochemistry 68 (2006) 206–212.
[67] J. Peng, C. Hou, X. Hu, Sens. Actuators B 169 (2012) 81–87.
[68] F.-C. Gong, X.-B. Zhang, C.-C. Guo, G.-L. Shen, R.-Q. Yu, Sensors 3 (2003) 91–100.